

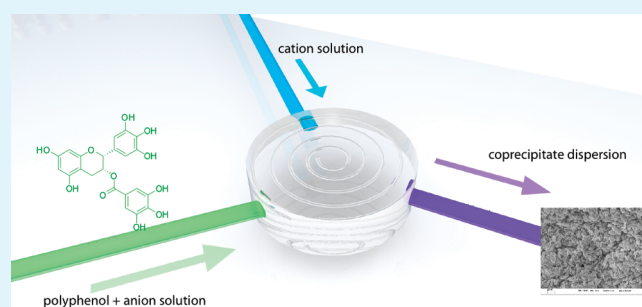
Selective Coprecipitation of Polyphenols in Bioactive/Inorganic Complexes

Amal Elabbadi, Nicolas Jeckelmann, Olivier Haefliger, Lahoussine Ouali, and Philipp Erni*

Firmenich SA, Corporate Research Division, 7 Rue de la Bergère, 1217 Meyrin 2 Genève, Switzerland

ABSTRACT: We investigate the formation of bioactive/inorganic coprecipitates of polyphenols catechins with calcium carbonate and calcium phosphate. Extracted from the leaves of *Camellia sinensis*, green tea catechins are efficient free radical scavengers, but their purported benefits from the perspective of prevention, health, and nutritional physiology are accompanied by unpleasant organoleptic characteristics: they are notoriously bitter. Selective complexation of polyphenols with metal salts is a possibility to mask or inactivate bitterness and/or off-flavors. We produce such complexes using a continuous coprecipitation process. With excess calcium chloride present in the matrix we observe a correlation of the carbonate to total anions molar ratio with the catechin load. To characterize the composition and structure of the coprecipitates we combine elemental analysis, scanning electron microscopy, X-ray powder diffraction, and liquid chromatography coupled to tandem mass spectroscopy (LC/MS-MS). We quantify the release kinetics in different model environments to predict the behavior of the catechins from the coprecipitates in model media simulating the conditions during oral ingestion and storage. The dissolution data suggest that the release profile of these delivery systems can be influenced and fine-tuned via the anion composition of the mineral carrier.

KEYWORDS: biomineralization, crystallization, chelation, antioxidants, flavonoids, delivery systems



INTRODUCTION

Tea, extracted from the plant *Camellia sinensis* and initially originating from China, is now the second most consumed beverage in the world after water.^{1–5} In addition to proteins, carbohydrates, and minerals, tea leaves contain polyphenols, a class of organic compounds composed of at least one benzene ring containing one or more hydroxyl groups; they are present in numerous plants and are known to be potent antioxidants.^{6,7} In particular, catechins are a subgroup of polyphenols comprising a common catechin backbone, from which other structures derive by hydroxyl and/or gallate moieties grafting. Their potential role as free radical scavengers in vivo and in vitro is of interest from the perspective of prevention, health and nutritional physiology.⁸ Accordingly, the concept of food fortification with green tea polyphenols has received considerable interest over the last years.^{9–13} Green tea has been extensively studied because of its high content in catechins.¹⁴ Additionally, polyphenols are used as antioxidants in various applications in food or consumer products.⁹ Unfortunately, the purported health or functional benefits of green tea polyphenols are accompanied by unpleasant organoleptic characteristics: they are notoriously bitter at typical concentrations relevant for nutritional fortification or as additives. Therefore, it would be desirable to mask or inactivate bitterness and/or off-flavors of green tea polyphenols without negatively affecting their structural integrity. Several studies have focused on the encapsulation of polyphenols to reduce or mask their bitterness: Kosaraju et al.¹⁵ described the encapsulation of different polyphenols extracts in caseinate/lecithin microcapsules by spray-drying. The

resulting microcapsules showed a good retention of the polyphenols' radical scavenging activity. Hu et al.¹⁶ reported on the encapsulation of tea catechins in ionically cross-linked tripolyphosphate/chitosan nanoparticles and demonstrated the feasibility of catechin release in vitro. Li et al.¹⁷ used electrospinning to produce protein fibers for stabilization of catechins. Polyphenols (tannic acid and tannins) were also shown to influence the mechanical and glass-transition properties of protein films.¹⁸ Kalogeropoulos et al.¹⁹ investigated the ability of β -cyclodextrin to form complexes and include polyphenols inside their cavity. The freeze-dried β -cyclodextrin/polyphenol complexes showed a good stability against thermal oxidation.

In our approach, described in this paper, we encapsulate green tea catechins in calcium phosphate/carbonate-based hybrid microparticles. Using mixed phosphate/carbonate matrices as host material offers numerous advantages. First, calcium phosphate (apatite) is itself an important source of nutrients, as it is a major component in bone mineral and in tooth enamel. In addition, the dissolution of this biodegradable material is strongly pH-dependent, and the release of the polyphenols may easily be triggered by gastric acid. Calcium phosphate and carbonate-based materials are extensively studied as model systems and in the field of biomineralization^{20–28} and tissue regeneration,²⁹ where the main interest lies in the preparation of composite

Received: May 4, 2011

Accepted: June 20, 2011

Published: July 07, 2011

Table 1. Composition of the Polyphenol and Anion Solutions Used for the Coprecipitation Experiments in the Presence of Excess Ca^{2+} ^a

anion solution (mol/L)			cation solution, CaCl_2 (mol/L)	polyphenol solution, GTE in acetic acid 0.01M	ratio carbonate to total anions, R_c (mol/mol)	ratio calcium to total anions, R_{ca} (mol/mol)
Na_2CO_3	Na_3PO_4	Na_2HPO_4				
0.000	0.100	0.100	0.4	20	0	2
0.050	0.075	0.075	0.4	20	0.25	2
0.100	0.050	0.050	0.4	20	0.50	2
0.160	0.020	0.020	0.4	20	0.80	2
0.200	0.000	0.000	0.4	20	1	2

^a For all compositions, blank samples were produced, corresponding to identical mineral composition in the absence of green tea polyphenols; GTE is the green tea extract raw material. All total concentrations in the anion solutions are kept constant at $c_{\text{carbonate}} + c_{\text{phosphates}} = 0.2$ mol/L and the degree of protonation of the phosphate species is 0.5 in all cases. This means the only parameter varied here is $R_c = c_{\text{carbonate}} / (c_{\text{carbonate}} + c_{\text{phosphates}})$, whereas all counterion solutions were prepared as aqueous calcium chloride solutions at a concentration of $c(\text{CaCl}_2) = 0.4$ mol/L, resulting in an excess calcium: total anions molar ratio $R_{ca} = c_{\text{Ca}^{2+}} / (c_{\text{carbonate}} + c_{\text{phosphates}}) = 2$ in all cases.

biopolymer/inorganic materials for bone defect repair. For instance, pectin hydrogels,³⁰ hyaluronic acid hydrogels,³¹ or collagen³² have been successfully mineralized with calcium phosphate for bone engineering. Likewise, inorganic silica surfaces were shown to have a good affinity for calcium phosphate and were used for the preparation of hybrid materials for the same purpose.^{33–35} Calcium phosphate was also discussed as a protein delivery system by Matsumoto et al.,³⁶ whereas calcium carbonate for encapsulating proteins was used as template for layer-by-layer deposition, followed by dissolution of the calcium carbonate core.³⁷ Butler et al.³⁸ investigated the crystallization of calcium carbonate in the presence of various gelling and nongelling biopolymers. Green et al.³⁹ described the encapsulation of various human cell types and growth factors in alginate/chitosan microcapsules mineralized with calcium phosphate and showed that the degree of mineralization of the polysaccharide microcapsules determined the delivery of the cells at the targeted site. Xu et al.⁴⁰ produced stable amorphous calcium carbonate microparticles stabilized by phytic acid. MacKenzie et al.²⁷ investigated the mechanisms for hierarchical growth of calcium carbonate in the presence of acidic glycoproteins from sea urchins. Finally, Fakhruddin et al.⁴¹ encapsulated individual living yeast cells in calcium carbonate microcapsules.

Our brief overview suggests that over the last years, interest has increased both in the oral delivery of polyphenols on one hand and, more generally, in the synthesis of mineral-based delivery systems on the other hand. Masking of green tea polyphenol bitterness is a real need, and although several delivery systems have been discussed in the literature, encapsulation of green tea polyphenols in coprecipitated bioactive/inorganic matrices has not yet received much attention.

Here, we report on the encapsulation of polyphenols (extracted from green tea leaves) in mixed calcium phosphate/calcium carbonate microparticles produced by a continuous coprecipitation process.^{42,43} By tuning the initial carbonate to phosphate molar ratio we attempt to reach high catechin loadings with a high encapsulation yield. In particular, it has previously been shown that catechins may be degraded considerably when the mineral matrix is rich in carbonate.⁴³ Here, we aim to stabilize the active ingredients across a wide range of anion carbonate and phosphate compositions by providing excess calcium chloride in the reactant solutions. We assess the role of the inorganic composition for the efficiency of polyphenol encapsulation in the presence of

excess calcium and characterize the stability of the coprecipitates as well as their release behavior in different model environments.

MATERIALS AND METHODS

Materials. Anhydrous calcium chloride (96%) and anhydrous dibasic sodium phosphate (>99%) were purchased from Acros Organics (Belgium). Trisodium phosphate hexahydrate from Fluka (Germany), sodium dihydrogen phosphate from Riedel-de Haën (Germany), sodium carbonate from VWR Prolabo (Belgium) and acetic acid from Carlo Erba (Italy) were used. Green tea extract (GTE) extracted from *Camellia sinensis* was purchased from Naturex, France. Water for LC/MS analysis was prepared using a Synergy 185 purification device (Millipore, Bedford, MA). LC/MS grade methanol was purchased from Merck (Darmstadt, Germany). Mass spectrometry grade formic acid was purchased from Fluka (Buchs, Switzerland).

Structural Characterization. Powder X-ray diffraction (XRD) spectra were recorded using a Stadi P diffractometer (Stoe & Cie GmbH, Germany). The radiation source used was a Ge (111) monochromator for Cu radiation yielding pure $K\alpha_1$ radiation. For SEM, the samples were dispersed in a droplet of water, placed onto the conducting slab and excess water was removed with a small piece of paper; prior to imaging the samples are dried in vacuum and sputter-coated with gold. Scanning electron microscopy (SEM) was performed on a LEO 1550-GEMINI instrument.

Compositional Analysis. Carbon, hydrogen, and nitrogen determinations were performed on an elemental analyzer (LECO CHN-800 analyzer, USA) by dry combustion followed by thermal conductivity measurement and infrared detection. Phosphorus was determined by inductively coupled plasma optical emission spectroscopy (ICP-OES) on an Optima 3000 DV spectrometer (Perkin-Elmer, Massachusetts). The water content was determined using the Karl Fischer method.

Quantification of Green Tea Polyphenols by LC/MS-MS. The LC/MS-MS method is an improved version⁴³ of an approach developed previously by Zeeb and co-workers.⁴⁵ Briefly, the coprecipitated samples were analyzed using a Shimadzu (Kyoto, Japan) UFLC XR chromatograph on a 150×2 mm Uptisphere-5 TF column (Interchim, Montluçon, France) and an Applied Biosystems/MDS Sciex (Concord, Canada) hybrid triple quadrupole/ion trap mass spectrometer. Data were reprocessed using Analyst 1.4.2 software. Full details for the specific parameter settings, calibration, and data analysis have been described elsewhere.⁴³

Coprecipitation Experiments. Hybrid catechin/inorganic particles were prepared using a continuous coprecipitation process based on double-inlet mixing cells.^{42,43} The setup consists of three peristaltic pumps (FEM 08 TT.18RC, KNF Flodos) and two PMMA mixing cells, connected

by silicone tubes. The phosphate/carbonate solution and the polyphenol solution were contacted in the first mixing cell at a flow rate of 2.5 mL/min each. The pH values of the reactant fluids were pH 8.9–11 for the anionic carbonate and phosphate solutions, pH 10.2 for the calcium chloride solution, and pH 3.15 for polyphenol/acetic acid solution. Then, the calcium solution was injected in the second mixing cell at the same flow rate to be brought in contact with the previous mixture and complete the coprecipitation, entrapping the polyphenols in the inorganic material. Immediately after precipitation, pH values in the slurries were in the range of pH 5.5–8. The resulting particles were collected at the outlet of the device and centrifuged during 3 min at 3500 rpm (2383 g). The solid phases were separated from the aqueous supernatants, which were acidified with 10 mmol of acetic acid in 100 mL volumetric flasks to avoid degradation of the nonencapsulated polyphenols in the supernatant. The solid precipitates were rinsed with 20 mL of Millipore water under sonication for 30 s and centrifuged again. The rinsing supernatants were immediately acidified with 2.5 mL of 0.1 M acetic acid and diluted to a volume of 25 mL with water. Blank samples were prepared by replacing the polyphenol solution with 0.01 M acetic acid. We performed coprecipitation experiments with varying carbonate:phosphate molar ratios $R_c = c_{\text{carbonate}} / (c_{\text{carbonate}} + c_{\text{phosphates}})$, where the carbonate and phosphate concentrations are in mol/L.

Here, calcium was always provided in excess ($c_{\text{Ca}^{2+}} = 0.4$ mol/L in the cation reactant solution), and each anion solution prepared contained a total $c_{\text{carbonate}} + c_{\text{phosphates}} = 0.2$ mol/L, where the carbonate is always Na_2CO_3 (at concentrations varying from $c_{\text{carbonate}} = 0$ –0.200 mol/L). This results in a total mineral concentration of 0.6 mol/L in the final slurry for all experiments. The phosphates are made up of Na_3PO_4 and Na_2HPO_4 at equimolar concentrations (at total phosphate concentrations from $c_{\text{phosphates}} = 0$ –0.200 mol/L). This protocol was developed based on the previous finding⁴³ that the loading was best for excess calcium (here: molar calcium to total anions ratio $R_{\text{ca}} = c_{\text{Ca}^{2+}} / (c_{\text{carbonate}} + c_{\text{phosphates}}) = 2$ in all cases), and a phosphate degree of protonation (based on reactant solution stoichiometry) of 0.5.

The resulting solids were redispersed in water and freeze-dried. All liquid phases were immediately analyzed by LC/MS-MS, either directly or after 1:10 dilution. The freeze-dried powders were dissolved in 1 M HCl in 10-mL volumetric flasks and filled to volume with Millipore water. The resulting solutions were analyzed by the same LC/MS-MS method either directly or after 1:10 dilution.

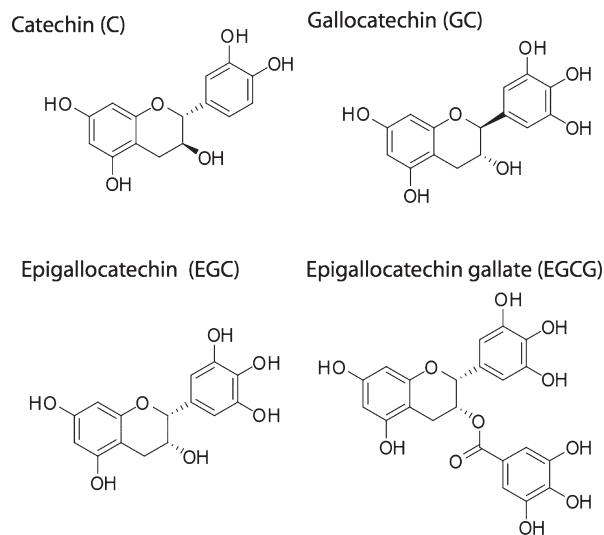
A stock solution of the green tea extract was prepared in 0.01 M acetic acid⁴⁴ (pH 3). For each coprecipitation experiment, a blank sample was prepared in the same conditions without the active. Among the samples with $R_c = 0.8$, additional samples were prepared with 8 g/L ascorbic acid in the polyphenol solution. An overview of the solutions used for the precipitation experiments is given in Table 1.

Dissolution Kinetics. Dissolution and release of the coprecipitated microparticles containing green tea polyphenols were evaluated in pH 6.8 phosphate buffer (NaH_2PO_4 0.1 M/ Na_2HPO_4 0.1 M, pH adjusted to 6.8 with a 1 M NaOH solution). The dissolution kinetics were recorded using a fiber-optic UV spectrometer (Ocean Optics Inc., Dunedin, FL, USA SD2000) equipped with a deuterium – halogen light source (Top sensor system DH-2000-FHS). The UV probe and a magnetic stirring bar were immersed in a beaker containing 50 mL of the phosphate buffer. The amount of freeze-dried sample corresponding to 1.7 mg total catechin content (calculated using the loadings obtained by LC/MS-MS) was dispersed therein, and data acquisition was initiated immediately. The dispersion was stirred magnetically during the experiment and the UV absorbance of the solution was measured in 2 s intervals at a wavelength of 274 nm, which is the absorbance maximum for the polyphenols used.

RESULTS AND DISCUSSION

We have previously shown that high loadings of green tea polyphenols in coprecipitated microparticles can be achieved,⁴³

Scheme 1. Known Molecular Structures of the Most Important Catechins Extracted from the Leaves of *Camellia sinensis*^{44–7}



^a They are based on a common catechin backbone; individual structures vary with respect to the presence of hydroxyl and/or gallate moieties and epi-forms. The abbreviations given between brackets are used in the text to indicate the different molecules.

and that at certain degrees of protonation of the phosphate species and at certain calcium:anion molar ratios the polyphenol loading in the particles attains a maximum value. With the combination of salt and catechin solutions of interest here, this was the case at a protonation degree of 0.5 ($c(\text{Na}_2\text{HPO}_4) = c(\text{Na}_3\text{PO}_4)$) and a calcium:anions molar ratio $R_{\text{ca}} = c_{\text{Ca}^{2+}} / (c_{\text{carbonate}} + c_{\text{phosphates}}) = 2$. Therefore, using these most favorable ratios, our objective here was to find the optimum combination of polyphenol complexation and carbonate/phosphate precipitation by varying $R_c = c_{\text{carbonate}} / (c_{\text{carbonate}} + c_{\text{phosphates}})$ from 0 to 1, i.e., by moving from pure phosphate precipitates to pure carbonate precipitates via mixtures of the two. To characterize the process and particles, we focus on the most important catechin species found in the leaves of *Camellia sinensis* (see Scheme 1 for examples): epigallocatechin gallate (EGCG), catechin gallate (CG), epicatechin gallate (ECG), epigallocatechin (EGC), gallo catechin gallate (GCG), gallo catechin (GC), epicatechin (EC), and catechin (C); these abbreviations will be used in the following.

Effect of the Carbonate:Total Anion Ratio on the Mass Balance in the Presence of Excess Calcium. We used LC/MS-MS analysis of the three phases resulting from the coprecipitation process (supernatant, rinsing water and the freeze-dried powder) to determine a mass balance, providing the loading $l = m_{\text{gp}} / m_{\text{p}}$, the encapsulation yield $y = m_{\text{gp}} / m_{\text{g0}}$, and the loss $p = 1 - (m_{\text{gs}} + m_{\text{gr}} + m_{\text{gp}}) / m_{\text{g0}}$. Here, m_{g0} is the mass of green tea extract initially added, m_{gs} is the mass of green tea polyphenols in the supernatant, m_{p} is the total mass of the powder, m_{gp} is the mass of green tea polyphenols in the powder, and m_{gr} is the mass of polyphenols measured in the water used for rinsing.

The evolution of the catechin loading, the encapsulation yield and the losses are represented in Figure 1 as a function of the anion stoichiometric ratio R_c . The loading in the powder systematically improved with increasing R_c . Likewise, the higher the carbonate content in the inorganic carrier, the higher the encapsulation yield:

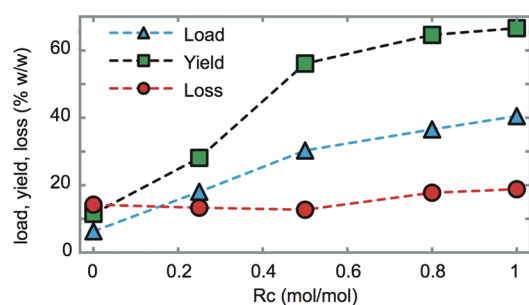


Figure 1. Influence of the anion stoichiometric ratio R_c on the polyphenol loading, encapsulation yield, and loss in the presence of excess Ca^{2+} for mixed mineral matrices (precursor solutions: $c(\text{CaCl}_2) = 2(c(\text{Na}_2\text{CO}_3) + c(\text{Na}_3\text{PO}_4) + c(\text{Na}_2\text{HPO}_4))$). Under these conditions, loads and yields remain stable at high R_c . The tracer considered for the LC/MS-MS determinations is EGCG.

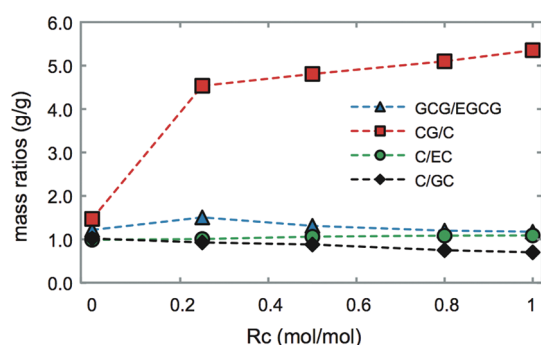


Figure 2. Selectivity of the coprecipitation toward gallated species, epi-forms and gallo-forms of catechins, and epi-forms of gallated species in the presence of excess Ca^{2+} for mixed mineral matrices (precursor solutions: $c(\text{CaCl}_2) = 2(c(\text{Na}_2\text{CO}_3) + c(\text{Na}_3\text{PO}_4) + c(\text{Na}_2\text{HPO}_4))$).

higher R_c values therefore favored encapsulation of green tea polyphenols in the mineral matrix. In contrast, the portion of catechins lost by degradation remained small, whatever the R_c value.

We have observed that with a 1:1 calcium:anion molar ratio and a protonation degree of 0.5, the catechin loading passes through a maximum at $R_c = 0.8$ and then dramatically drops as R_c is increased further;⁴³ in other words, catechins are degraded considerably at high values of R_c due to the high pH inherent to anion compositions rich in carbonate.⁴³ Here, we attempt to achieve better stability by providing excess calcium chloride in the precursor solutions. The calcium:anion molar ratio was set to 2 while the R_c value was varied from 0 to 1, and the protonation degree was retained at 0.5. Indeed, Figure 1 demonstrates that increased loadings are obtained even at the highest R_c values. This key result suggests that excess calcium stabilizes the catechins and/or enhances their availability for precipitation-based encapsulation at high carbonate content. It is possible that the excess of calcium and its important role in the formation of amorphous calcium carbonate, as it is known from biomineralization,⁴⁶ positively influences the precipitation of calcium/polyphenol complexes at the expense of crystalline calcium carbonate; we will address this hypothesis below using X-ray powder diffraction.

Selectivity of Polyphenol/Inorganic Coprecipitation. Figure 2 demonstrates the encapsulation selectivity of the coprecipitation method for different catechin species. A comparison of the loading determined for different polyphenol tracers suggests

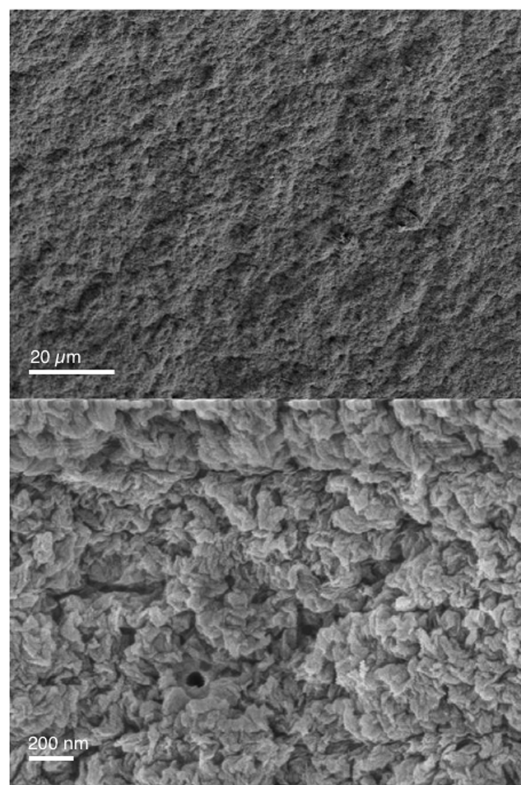


Figure 3. Typical scanning electron micrographs of amorphously coprecipitated, mixed polyphenol/mineral complexes; $c_{\text{phosphate}} = 0.07$ mol/L, $c_{\text{carbonate}} = 0.03$ mol/L.

strong variations in affinity between the inorganic carriers and individual polyphenols. For instance, the ratio GCG/EGCG is the proportion of the *epi*-configuration of a gallated species; the ratio CG/C compares the relative amount of the galloyl moiety; the ratio C/EC reflects the presence of the *epi*-configuration of nongallated species, and the ratio C/GC quantifies the effect of the gallo-group. Most importantly, CG/C was far above unity when $R_c > 0$. This key result indicates that the coprecipitation process was selective toward the gallated species as compared to their nongallated counterparts. In the example shown in Figure 2, gallo catechin exceeded catechin up to a factor 5 by mass. In contrast, neither the epimer configuration nor the gallo-group influenced the encapsulation efficiency, as shown by the ratios GCG/EGCG ≈ 1 , C/EC ≈ 1 , and C/GC ≈ 1 at any R_c value.

The continuous precipitation process using the double-inlet flow cells provides stable, reproducible reaction conditions. For example, eight replicates of a sample with $R_c = 0.8$ were produced (data not shown) and their average EGCG loading determined by LC/MS-MS was $39.8 \pm 2.6\%$. The topography of the samples (Figure 3) indicates that they are constituted of agglomerated units having an average size of 60–80 nm. Besides the size of the typical primary particles, the micrographs demonstrate the strong effect of anion stoichiometry on the aggregation state of the coprecipitates. The SEM images of particles indicate a mostly amorphous morphology; green tea polyphenols seem to inhibit classical crystallization of carbonate or phosphate salts. This result is reminiscent of the amorphous, stable CaCO_3 microparticles formed in the presence of phytic acid, as prepared by Xu and co-workers⁴⁰ using a gas-diffusion method. More generally, morphology development and controlled, nonclassical crystallization in the

presence of additives has recently attracted much attention, especially from the perspective of biomineralization.^{47,48} The primary particle size for types of precipitates is well-defined, and is typically in the range of 60–80 nm. Their assembly into micrometer-sized and larger particles appears to be influenced by the distribution of charges on the particles and due to nonprecipitated electrolytes in the suspension, and by colloidal stabilization of both the primary particles and their aggregates by both coprecipitated and free polyphenols. We expect that all of these factors depend on the particular formulation, resulting in different aggregation states of the material.

XRD Patterns for Polyphenol/Calcium Carbonate and Polyphenol/Calcium Phosphate Coprecipitates. Powder XRD patterns were collected to study the differences in crystallinity obtained with different mineral matrices. Again, the calcium:anion molar ratio was held constant at 2 in both cases. In Figure 4 we compare the spectra of the coprecipitated particles with their blank counterparts for the cases calcium carbonate and calcium phosphate/dicalcium phosphate matrices. The carbonate-only system ($R_c = 1$), more highly loaded with polyphenols, was predominantly amorphous as indicated by the absence of sharp peaks and the wavy baseline. In contrast, the pattern for $R_c = 0$ was merely attenuated in the presence of catechins, with both the mineral blank and the coprecipitates exhibiting identical peaks with comparable relative magnitudes. This similarity

suggests that either the amount of polyphenols present in the particles at $R_c=0$ is insufficient to significantly inhibit crystallization, and/or that calcium phosphate/dicalcium phosphate crystallization is less susceptible to inhibition by polyphenols. We also point out that mixing different anionic species already has an effect on the crystallization behavior, independent of the presence of polyphenols.⁴³ Inclusion of catechins in the mixed and pure carbonate particles appears to have an inhibitory effect on the crystallization of the inorganic material, but the effect appears to be strongest for $R_c = 1.0$ (carbonate only), where the sample is mostly amorphous; in contrast, for $R_c = 0$ (phosphates only), the polyphenols do not strongly suppress crystallization.

Elemental Analysis. We performed elemental analysis of carbon, hydrogen, nitrogen, calcium, phosphorus and measured the water content to determine the chemical composition of the coprecipitates. Because the carbon content in the product can stem from either the carbonate anions or the catechins, we first determined the chemical formulas of the blank samples. We assumed that the composition of the inorganic material was the same in the coprecipitated particles and in their blank counterparts and attributed the exceeding carbon in the loaded particles to the catechins. For simplicity, we assumed that EGCG is the predominant polyphenol. This way, the amount of polyphenols can be estimated and compared with the LC/MS-MS results. Additionally, the electroneutrality of the resulting precipitates was also verified. Table 2 displays the formulas determined for the three polyphenol-free mineral matrices, and highlights the differences between the nominal R_c values based on the solution concentrations and the actual R_c in the product obtained by elemental analysis. The variation between the two values indicates a competition between the carbonate ions and the phosphate ions during the precipitation process. The higher the nominal R_c value, the lower the relative variation and the better the agreement between the nominal and actual values. For low carbonate content ($c_{\text{phosphate}} > c_{\text{carbonate}}$), we expect a competition between the carbonate and the phosphate species during formation of the microparticles. At high R_c , this effect becomes insignificant. At low R_c , the predominating phosphate species are preferentially included in the inorganic microparticles as compared to the carbonate. Indeed, a comparison of the solubility

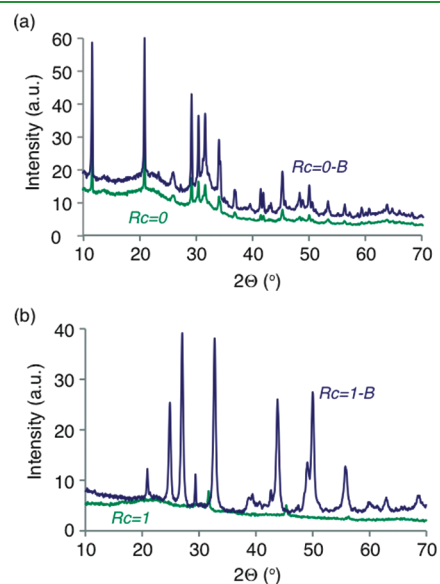


Figure 4. XRD spectra of polyphenol/mineral coprecipitates prepared with excess Ca^{2+} ; (a) phosphate only ($R_c = 0$ and $c(\text{Na}_2\text{HPO}_4) = c(\text{Na}_3\text{PO}_4) = 0.1$ mol/L in the reactant solution), (b) carbonate only ($R_c = 1$, $c(\text{Na}_2\text{CO}_3) = 0.2$ mol/L in the reactant solution). Both the catechin/inorganic coprecipitates and their corresponding blank (mineral-only, “-B”) counterparts are included. The intensity is plotted in arbitrary units (a.u.) against the scattering angle 2θ .

Table 3. Evaluation of the Polyphenol Content in the Samples with $R_c = 0.25, 0.50$, and 0.80 Based on Carbon Determination and Comparison with the LC/MS-MS Determination, Based on Epigallocatechin Gallate (EGCG) as the Tracer

	R_c		
	0.25	0.50	0.80
polyphenol content, elemental analysis (wt %)	18.3	27.0	34.5
polyphenol content, LC/MS-MS based on EGCG (wt %)	18.0	30.3	35.3

Table 2. Determination of the Stoichiometry of the Precipitated Blank (inorganic) Microparticles by Elemental Analysis; Difference between the Nominal and Actual R_c Values

nominal R_c (mol/mol)	actual R_c (mol/mol)	hypothetical formula	charge balance
0.25	0.103	$\text{Ca}(\text{PO}_4)_{0.65}(\text{CO}_3)_{0.075} \cdot 0.97 \text{H}_2\text{O}$	$2 - (3 \cdot 0.65) - (2 \cdot 0.075) = 0$
0.50	0.368	$\text{Ca}(\text{PO}_4)_{0.48}(\text{CO}_3)_{0.28} \cdot 0.97 \text{H}_2\text{O}$	$2 - (3 \cdot 0.48) - (2 \cdot 0.28) = 0$
0.80	0.764	$\text{Ca}(\text{PO}_4)_{0.21}(\text{CO}_3)_{0.68} \cdot 0.62 \text{H}_2\text{O}$	$2 - (3 \cdot 0.21) - (2 \cdot 0.68) = 0$

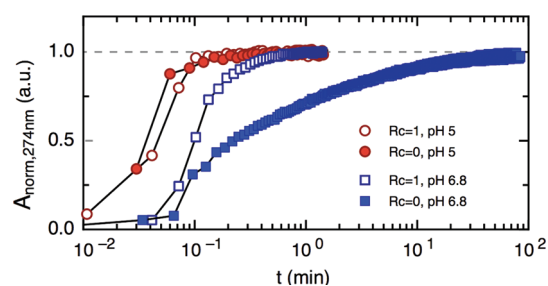


Figure 5. pH-responsive release: dissolution profiles of the catechin/inorganic coprecipitates with varying anion composition at two different pH values. Normalized absorption at a wavelength of 274 nm measured by UV/vis spectroscopy. Lines guide the eye.

products of calcium carbonate ($K_{sp}(\text{CaCO}_3) \approx 1 \times 10^{-9}$) and calcium phosphate ($K_{sp}(\text{Ca}_3(\text{PO}_4)_2) \approx 1 \times 10^{-26}$) indicates that the calcium phosphate was formed preferentially and was more stable than calcium carbonate. Table 3 summarizes the catechin loadings calculated from the carbon determination and compares the results with the LC/MS-MS determinations previously obtained, indicating excellent correlation between the loading results obtained by elemental analysis and by LC/MS-MS. This agreement supports our hypothesis that the composition of the mineral carrier is similar in the catechin-loaded particles and in the blank inorganic matrices.

Evaluation of the Release Kinetics and Stability. The release profile of the coprecipitated microparticles was evaluated using UV-spectroscopy. We quantified pH-controlled release under two different conditions at pH 6.8, where we expected the particles to remain relatively stable against dissolution, and at pH 5, where rapid dissolution and complete release of the active should occur. The measurements were performed at the absorbance maximum of the green tea polyphenols, determined to be at 274 nm. Figure 5 shows the release profile from the hybrid particles at two different anion stoichiometric ratios. The particles made of pure carbonate released their total amount of polyphenols within tens of seconds, independent of the pH value, since calcium carbonate, which constituted the mineral matrix for $R_c = 1$, dissolves more easily at neutral pH. This behavior suggests that pure carbonate particles are suitable if the active is to be released during oral ingestion (release at neutral pH during seconds to tens of seconds); however, if the goal is to keep the active at least partially encapsulated during oral ingestion, the calcium carbonate matrices produced here dissolve too quickly. In contrast, the particles containing calcium phosphate carrier were far less soluble at neutral pH.^{49,50} In this case (here, $R_c = 0$), the release at neutral pH occurred gradually over 15 min; exposing the identical particles to a lower pH again led to more rapid release. Therefore, mixed carbonate/phosphate or phosphate-based particles may be suitable if the dissolution during oral consumption has to be minimized and subsequent release in acidic conditions is desired. The difference in dissolution behavior for inorganic matrices composed of different salts suggests that the dissolution behavior of the coprecipitates can easily be controlled via the anion stoichiometric ratios in the initial solutions.

To assess the effectiveness of precipitated mineral particles as delivery systems, it is important to understand the behavior under typical storage conditions, both for the entirety of polyphenols and for the individual species. We exposed the lyophilized precipitates

to various storage conditions. Figure 6 summarizes the evolution of the polyphenol content under anaerobic conditions (the samples were held under argon atmosphere and isolated from light) over the course of 60 days. The evolution of the relative content in selected tracers as compared to the loading in the freshly prepared microparticles is plotted at 23 °C and at -18 °C, using different polyphenol tracers. These curves suggest that the coprecipitation process, along with a decrease in temperature, reduces and delays degradation across all polyphenol tracers investigated, and up to 70% of the initial polyphenols remain intact at the end of the stability tests. The most sensitive compounds are polyphenols having a galloyl group, such as EGCG and GCG. Identical tests were also performed in air instead of argon but did not reveal any significant differences, indicating that storage under aerobic conditions did not affect sample degradation. Similarly, photodegradation under aerobic conditions was excluded as a factor influencing the long-term stability of the polyphenols within the precipitates. In contrast, the storage temperature is a key parameter for the chemical stability of the encapsulated polyphenols, as shown in Figure 6: under low-temperature conditions, we observed not only a retention in total polyphenols content over extended times but also reduction in selective degradation for individual species; Figure 6 suggests that the encapsulation process along with a decrease in temperature efficiently reduces and delays degradation for individual polyphenols. The gallated species (EGCG and GCG) are the most sensitive to degradation, and probably to hydrolysis of the galloyl moiety. On the other hand, the level of EGC remained high, whereas the amount of GC dropped. This may be due to the epimerization of the GC, transforming it into EGC. The effect of ascorbic acid was evaluated with respect to its reported stabilizing capacity against catechin degradation.⁵¹ Contrary to results presented by Chen et al.⁵¹ for simple solutions of green tea polyphenols, the addition of ascorbic acid did not improve the storage stability: its reported stabilizing effect in fresh solutions apparently does not translate into sustained stabilization in the precipitated mineral matrices investigated here over extended storage times.

SUMMARY AND CONCLUSIONS

Our objective was to design and characterize a delivery system for catechins from green tea based on their coprecipitation with salt solutions to form hybrid particles. Catechin-loaded inorganic/bioactive particles were formed by contacting sodium phosphate/sodium carbonate and calcium chloride precursor solutions in the presence of the polyphenols in aqueous solution. The rapid continuous precipitation process using the double inlet flow cells provides stable, reproducible reaction conditions and avoids extended exposure of the catechins to unfavorable medium conditions that could lead to degradation. Screening the carbonate to total anions ratio, we found that the higher the carbonate content in the inorganic material, the higher the polyphenol loading and the better the encapsulation yield. Moreover, increasing the carbonate content did not induce polyphenol degradation, presumably due to the presence of excess Ca^{2+} stabilizing the polyphenols.

The specific nature of the interactions between the catechins, calcium cations, and/or intermediate nanoscale precursors of the particles formed during precipitation is a topic that needs further investigation. Chelation of polyphenols and the formation of metal-polyphenol complexes has been studied and discussed^{52,53} for iron(III), iron(II), copper(II), zinc(II), and aluminum(III); however, those authors specifically pointed out that polyphenols

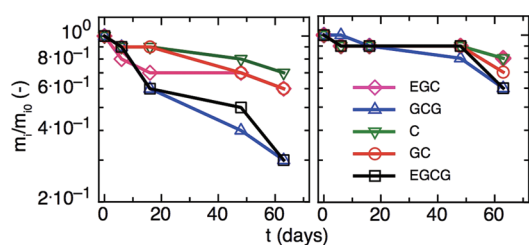


Figure 6. Temporal evolution of the polyphenol content (samples held under argon atmosphere and isolated from light). The ratios m_t/m_0 between the polyphenol loading after a given time t and the loading in the freshly prepared microparticles are plotted at 23 °C (left) and at -18 °C (right), using different polyphenol tracers (EGCG, EGC, GC, GCG, C).

do not chelate alkali and alkaline earth cations (Na^+ , K^+ , Ca^{2+}). They also argue that in the case of Mg^{2+} , there might be some weak interaction with polyphenols, which is, however, expected to be negligible in competition with phosphate. Besides, ionic interactions with cations in the reactant solutions, it is worth assessing interactions of polyphenols with the surfaces of the nascent (co)precipitates. In the framework of nonclassical crystallization,²⁰ polyphenols may well play a role similar to phytic acid⁴⁰ (inositol hexakisphosphate), which has been argued to act not only as a crystallization inhibitor in the formation of amorphous CaCO_3 , but also as a colloidal stabilizer of the primary precipitated nanoparticles as they undergo mesoscale assembly.

XRD spectra of the samples with the highest loadings indicated a mostly amorphous structure in the coprecipitates. The encapsulation process along with a decrease in temperature efficiently reduces and individually delays degradation with up to 70% of the initial polyphenols remaining intact at the end of the stability tests. The most sensitive compounds are polyphenols having a galloyl group, such as EGCG and GCG. We also demonstrated that the dissolution and release kinetics can be influenced via the anion composition of the mineral carrier. This allows the design of delivery systems with rapid, pH-triggered release upon contact with an acidic environment but only slow and gradual dissolution at neutral pH. Using appropriate ion compositions, the time window of release can be optimized to be anywhere between a few seconds up several minutes. A possible application is the masking or inactivation of bitterness and/or off-flavors of green tea polyphenols⁵⁴ while minimizing degradation.

AUTHOR INFORMATION

Corresponding Author

*E-mail: philipp.erni@firmenich.com.

ACKNOWLEDGMENT

We cordially thank Mrs Céline Besnard (University of Geneva) for the XRD data acquisition and Dr. Andreas Herrmann (Firmenich) for helpful comments on the manuscript. Rona Pitschke is acknowledged for help with the SEM experiments.

REFERENCES

- (1) Marcos, A.; Fisher, A.; Rea, G.; Hill, S. J. *J. Anal. At. Spectrom.* **1998**, *13*, 521–526.
- (2) Barroso, M. B.; van de Werken, G. J. *High Res. Chromatogr.* **1999**, *22*, 225–230.

- (3) Khokhar, S.; Magnúsdóttir, S. G. M. *J. Agric. Food Chem.* **2002**, *50*, 565–570.
- (4) Friedman, M.; Levin, C. E.; Choi, S. H.; Kosukue, E.; Kosukue, N. *J. Food Sci.* **2006**, *71*, C328–C337.
- (5) Wang, Y.; Ho, C. T. *J. Agric. Food Chem.* **2009**, *57*, 8109–8114.
- (6) Handique, J. G.; Baruah, J. B. *React. Funct. Polym.* **2002**, *52*, 163–188.
- (7) Quideau, S.; Deffieux, D.; Douat-Casassus, C.; Pouységu, L. *Angew. Chem., Int. Ed.* **2010**, *50*, 586–621.
- (8) Higdon, J. V.; Frei, B. *Crit. Rev. Food Sci. Nutr.* **2003**, *43*, 89.
- (9) Lomova, M. V.; Sukhorukov, G. B.; Antipima, M. N. *ACS Appl. Mater. Interface* **2011** article in press.
- (10) Shutava, T. G.; Balkundi, S. S.; Vangala, P.; Steffan, J. J.; Bigelow, R. L.; Cardelli, J. A.; O'Neal, D. P.; Lvov, Y. M. *ACS Nano* **2009**, *3*, 1877–1885.
- (11) Shutava, T. G.; Balkundi, S. S.; Lvov, Y. M. *J. Colloid Interface Sci.* **2009**, *330*, 276–283.
- (12) Sies, H. *Arch. Biochem. Biophys.* **2010**, *501*, 2–5.
- (13) Verhagen, H.; Vos, E.; Francl, S.; Heinonen, M.; van Loveren, H. *Arch. Biochem. Biophys.* **2010**, *501*, 6–15.
- (14) Yokozawa, T.; Dong, E.; Nakagawa, T.; Kashiwagi, H.; Nakagawa, H.; Takeuchi, S.; Chung, H. Y. *J. Agric. Food Chem.* **1998**, *46*, 2143–2150.
- (15) Kosaraju, L. S.; Labbett, D.; Emin, M.; Konczak, I.; Lundin, L. *Nutr. Diet.* **2008**, *65*, S48–S52.
- (16) Hu, B.; Sun, Y.; Hou, Z.; Ye, H.; Zeng, X. *J. Agric. Food Chem.* **2008**, *56*, 7451–7458.
- (17) Li, Y.; Lim, L. T.; Kakuda, Y. *J. Food Sci.* **2009**, *74*, C233–C240.
- (18) Emmambux, M. N.; Stading, M.; Taylor, J. R. N. *J. Cereal Sci.* **2004**, *40*, 127–135.
- (19) Kalogeropoulos, N.; Yannakopoulou, K.; GiOXari, A.; Chiou, A.; Makris, D. P. *Food Sci. Technol.* **2010**, *43*, 882–889.
- (20) Cölfen, H.; Antonietti, M. *Mesocrystals and Nonclassical Crystallization: New Self-Assembled Structures*; Wiley-Blackwell: Chichester U.K., 2008.
- (21) Cölfen, H. *Curr. Opin. Colloid Interface Sci.* **2003**, *8*, 23–31.
- (22) DiMasi, E.; Kwak, S. Y.; Amos, F. F.; Olszta, M. J.; Lush, D.; Gower, L. B. *Phys. Rev. Lett.* **2006**, *97*, 045504.
- (23) Meldrum, F.; Cölfen, H. *Chem. Rev.* **2008**, *108*, 4332–4432.
- (24) Maas, M.; Guo, P.; Keeney, M.; Yang, F.; Hsu, T. M.; Fuller, G. G.; Martin, C. R.; Zare, R. N. *Nano Lett.* **2011**, *11*, 1383–1388.
- (25) Maas, M.; Rehage, H.; Nebel, H.; Epple, M. *Langmuir* **2009**, *25*, 2258–2263.
- (26) Xu, G.; Aksay, I. A.; Groves, J. T. *J. Am. Chem. Soc.* **2001**, *123*, 2196–2203.
- (27) MacKenzie, C. R.; Wilbanks, S. M.; McGrath, K. M. *J. Mater. Chem.* **2004**, *14*, 1238–1244.
- (28) Lendrum, C. D.; McGrath, K. M. *Cryst. Growth Des.* **2009**, *9*, 4391–4400.
- (29) Dorozhin, S. V.; Epple, M. *Angew. Chem., Int. Ed.* **2002**, *41*, 3130–3146.
- (30) Ichibouji, T.; Miyazaki, M.; Ishida, E.; Sugino, A.; Ohtsuki, C. *Mater. Sci. Eng., C* **2009**, *29*, 1765–1769.
- (31) Morita, Y.; Matsumoto, C.; Miyazaki, T.; Ishida, E.; Tanaka, K.; Goto, T. *Trans. Mater. Res. Soc. Jpn.* **2009**, *34*, 85–87.
- (32) Nassif, N.; Gobeaux, F.; Seto, J.; Belamie, E.; Davidson, P.; Panine, P.; Mosser, G.; Fratzl, P.; Giraud Guille, M. M. *Chem. Mater.* **2010**, *22*, 3307–3309.
- (33) Ohtsuki, C.; Kokubo, T.; Yamamuro, T. *J. Non-Cryst. Solids* **1992**, *143*, 84–92.
- (34) Yokoi, T. *J. Mater. Res.* **2009**, *24*, 2154–2160.
- (35) Hashizume, M.; Horii, H.; Kikuchi, J. I.; Kamitakahara, M.; Ohtsuki, C.; Tanihara, M. *J. Mater. Sci. Mater. Med.* **2009**, *21*, 11–19.
- (36) Matsumoto, T.; Okazaki, M.; Inoue, M.; Yamaguchi, S.; Kusunose, T.; Toyonaga, T.; Hamada, Y.; Takahashi, J. *Biomaterials* **2004**, *25*, 3807–3812.
- (37) Petrov, A. I.; Volodkin, D. V.; Sukhorukov, G. B. *Biotechnol. Prog.* **2005**, *21*, 918–925.

- (38) Butler, M. F.; Glaser, N.; Weaver, A. C.; Kirkland, M.; Heppenstall-Butler, M. *Cryst. Growth Des.* **2006**, *6*, 781–794.
- (39) Green, D. W.; Levêque, I.; Walsh, D.; Howard, D.; Yang, X.; Partidge, K.; Mann, S.; Oreffo, R. O. C. *Adv. Funct. Mater.* **2005**, *15*, 1–7.
- (40) Xu, A. W.; Yu, Q.; Dong, W. F.; Antonietti, M.; Cölfen, H. *Adv. Mater.* **2005**, *17*, 2217–2221.
- (41) Fakhrullin, R. F.; Minullina, R. T. *Langmuir* **2009**, *25*, 6617–6621.
- (42) Peytcheva, A.; Cölfen, H.; Schnablegger, H.; Antonietti, M. *Colloid Polym. Sci.* **2002**, *280*, 218–227.
- (43) Elabbadi, A.; Jeckelmann, N.; Haefliger, O. P.; Ouali, L. *J. Microencapsulation* **2011**, *28*, 1–9.
- (44) Zhu, Q. Y.; Zhang, A.; Tsang, D.; Huang, Y.; Chen, Z. Y. *J. Agric. Food Chem.* **1997**, *45*, 4624–4628.
- (45) Zeeb, D. J.; Nelson, B. C.; Albert, K.; Dalluge, J. J. *Anal. Chem.* **2000**, *72*, 5020.
- (46) Gower, L. *Chem. Rev.* **2008**, *108*, 4551.
- (47) Pouget, E. M.; Dujardin, E.; Cavalier, A.; Moreac, A.; Valéry, C.; Marchi-Artzner, V.; Weiss, T.; Renault, A.; Paternostre, M.; Artzner, F. *Nat. Mater.* **2007**, *6*, 434.
- (48) Pouget, E. M.; Bomans, P. H. H.; Dey, A.; Frederik, P. M.; de With, G.; Sommerdijk, N. A. J. M. *J. Am. Chem. Soc.* **2010**, *132*, 11560.
- (49) Schiller, C.; Epple, M. *Biomaterials* **2003**, *24*, 2037–2043.
- (50) Shellis, R. P.; Lee, A. R.; Wilson, R. M. *J. Colloid Interface Sci.* **1999**, *218*, 351–358.
- (51) Chen, Z. Y.; Zhu, Q. Y.; Wong, Y. F.; Zhang, Z.; Chung, H. Y. *J. Agric. Food Chem.* **1998**, *46*, 2512–2516.
- (52) Hider, R. C.; Liu, Z. D.; Khodr, H. H. *Method. Enzymol.* **2001**, *335*, 190–203.
- (53) Brown, J. E.; Khodr, H.; Hider, R. C.; Rice-Evans, C. A. *Biochem. J.* **1998**, *330*, 1173.
- (54) Zeng, Q. C.; Wu, A. Z.; Pika, J. J. *Breath Res.* **2010**, *4*, 036005.